Photon Blockade with Ground-State Neutral Atoms

A. Cidrim,[1] T. S. do Espirito Santo,[2] J. Schachenmayer,[3] R. Kaiser,[4] and R. Bachelard[1,4]
[1]Departamento de Física, Universidade Federal de São Carlos, Rod. Washington Luís, km 235—SP-310, 13565-905 São Carlos, SP, Brazil
[2]Instituto de Física de São Carlos, Universidade de São Paulo—13560-970 São Carlos, SP, Brazil
[3]IPCMS (UMR 7504) and ISIS (UMR 7006), Université de Strasbourg, CNRS, 67000 Strasbourg, France
[4]Université de Côte d'Azur, CNRS, Institut de Physique de Nice, 06560 Valbonne, France

(Received 30 April 2020; accepted 13 July 2020; published 13 August 2020)

We show that induced dipole-dipole interactions allow for photon blockade in subwavelength ensembles of two-level, ground-state neutral atoms. Our protocol relies on the energy shift of the single-excitation, superradiant state of N atoms, which can be engineered to yield an effective two-level system. A coherent pump induces Rabi oscillation between the ground state and a collective bright state, with at most a single excitation shared among all atoms. The possibility of using clock transitions that are long-lived and relatively robust against stray fields, alongside new prospects on experiments with subwavelength lattices, makes our proposal a promising alternative for quantum information protocols.

DOI: 10.1103/PhysRevLett.125.073601

Photon-induced blockade is a mechanism where multiexcitation states become marginally populated owing to a nonlinearity in the excitation spectrum, e.g., due to energy shifts caused by interactions. In atomic systems, it has been achieved up to date using Rydberg atoms, excited to highly energetic levels, with a principal quantum number of several tens [1–4]. Crucially, such setups rely on huge attainable interaction strengths among Rydberg excited atoms, which can be many orders of magnitude larger than other typical interaction strengths (e.g., involving van der Waals or magnetic dipole-dipole forces) of the ground states. The resulting interaction translates into a strong repulsion between two Rydberg atoms, which shifts the multiexcitation states in energy [see Fig. 1(a)] and can block the presence of more than one excitation inside the so-called blockade radius. Through this mechanism, it is thus possible to address a single-excitation "superatom" state of N atoms (typically a symmetric state). This allows one to simulate an effective two-level system, consisting of a collective excited state of the form $|\psi_s\rangle = (1/\sqrt{N})\sum_{i=1}^{N} e^{i\mathbf{k}\cdot\mathbf{r}_i}|g\ldots g e_i g\ldots g\rangle$ (with $\mathbf{k}$ the pump wave vector and $\mathbf{r}_i$ the position of atom i) and a ground state $|\psi_g\rangle = (1/\sqrt{N})|g\ldots g\rangle$. The coupling to the pump with single-atom Rabi frequency Ω results in the collective Rabi oscillations at frequency $\sqrt{N}\Omega$. They are the hallmark of photon blockade, as they provide a direct observable of the collective state, and serve as a witness of the N-atom entanglement. Indeed, starting from ground-state atoms and switching off the pump after a quarter of the collective oscillation fully populates the entangled state $|\psi_s\rangle$. Other signatures, possibly less easily accessible experimentally, are the excitation number of the system, as well as the correlation functions between neighboring atoms, that shows the suppression of two excitations to be within the same blockade radius. This mechanism makes experiments with Rydberg states of neutral atoms attractive platforms to implement quantum information protocols [1,2].

While Rydberg physics can be ideal for the generation of appreciable quantum correlations and entanglement, there can be several downsides of using such systems, which usually stem from challenging experimental control levels. For instance, these atomic states are extremely sensitive to stray electric and magnetic fields due to their large dipole moments [5,6]. Furthermore, it has been shown that the dense spectrum of nearby Rydberg states might severely

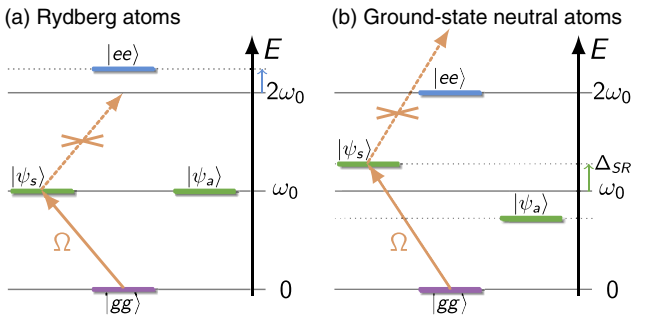

FIG. 1. Transition scheme for a pair of atoms (a) in a Rydberg configuration, where the energy shift occurs for the doubly excited state, the symmetric state is directly addressed using the atomic transition wavelength. (b) In a configuration with strong induced dipole-dipole interactions, the energy of symmetric and antisymmetric single-excitation states shifts oppositely: in this case, to target the symmetric state, the pump is detuned by the interaction-induced shift Δ_{SR}.

shorten the time available for coherent manipulation of the Rydberg atoms, implying restrictions to protocols that involve dressing states, for instance [7]. Additionally, their excitation is often realized through a two-photon process, which in turn induces losses during the commonly used stimulated Raman adiabatic passage. We note, however, that recent experiments using ultrafast pulses have achieved remarkable coherent control of Rydberg states in very short times [8,9]. In this context, an alternative scheme using ground-state neutral atoms to study many-body spin systems could bring the benefits from long-lived transitions. In particular, their lesser sensitivity to stray fields, from which atomic clocks strongly benefit [10], would translate into more robustness for coherent control.

Here we consider instead the case of ground-state neutral atoms that interact solely through induced dipole-dipole interactions and have a simple two-level internal structure. While Rydberg states result in effectively micrometer-sized atoms, in order to reach strong enough interaction strengths in our system we consider subwavelength samples. Such systems have recently drawn considerable attention, as dipole-dipole interactions at short distances can generate spin squeezing [11] and also extraordinary subradiance, allowing for long-lived entangled states that may eventually behave as quantum memories [12–18]. Despite the trapping and coherent manipulation of atoms at scales below the diffraction limit being experimentally challenging, seminal theoretical proposals based on the dark states of electromagnetically induced transparency have paved the way to surpass this limitation [19–22]: they have been successfully applied, for example, to ultraprecise localization of atomic excitations [23] and to the generation of subwavelength potentials for cold atoms [24–26].

Although our proposal presents similar physics to the Rydberg blockade, it differs in the fact that the shift in energy occurs not on a highly excited state, but rather on the single-excitation states. The simple case for $N = 2$ is depicted in Fig. 1(b) and contrasted with the Rydberg counterpart. Here we address the detuned symmetric state by setting the pump frequency to $\omega_0 + \Delta_{\mathrm{SR}}$, with ω_0 the bare single-atom transition frequency. This frequency shift Δ_{SR} prevents populating the two-excitation state, inducing a blockade mechanism.

We consider a linear chain of N two-level atoms excited with a linear polarization orthogonal to the chain, so the induced electric dipoles couple through the exchange of real and virtual photons. Their dynamics is described (under both Markov and rotating-wave approximation) by a quantum master equation of the form ($\hbar \equiv 1$) [27–29]

$$\frac{d}{dt}\hat{\rho} = -\mathrm{i}[\hat{H}, \hat{\rho}] + \mathcal{L}(\hat{\rho}), \tag{1}$$

where the coherent Hamiltonian dynamics is given by

$$\hat{H} = -\Delta \sum_i \hat{\sigma}_i^+ \hat{\sigma}_i^- + \frac{1}{2}\sum_i (\Omega e^{i\mathbf{k}\cdot\mathbf{r}_i}\hat{\sigma}_i^+ + \mathrm{H.c.}) + \sum_{i,j} \Delta^{ij} \hat{\sigma}_i^+ \hat{\sigma}_j^-, \tag{2}$$

whereas the Lindbladian part reads

$$\mathcal{L}(\hat{\rho}) = \frac{1}{2}\sum_{i,j} \Gamma^{ij}(2\hat{\sigma}_i^- \hat{\rho} \hat{\sigma}_j^+ - \{\hat{\sigma}_j^+ \hat{\sigma}_i^-, \hat{\rho}\}). \tag{3}$$

We assume that our system is being pumped by a laser with Rabi frequency Ω and detuned by Δ from ω_0. The dipole-dipole nature of the interaction is embedded in the assumption of pointlike dipoles whose associated Green's tensor is given by $\mathbf{G}_{ij} \equiv \mathbf{G}(\mathbf{r}_{ij}) = (3\Gamma/4)\{[e^{ikr_{ij}}]/(kr_{ij})^3\}[(k^2 r_{ij}^2 + ikr_{ij} - 1)\mathbb{1}_3 - (k^2 r_{ij}^2 + i3kr_{ij} - 3)(\mathbf{r}_{ij}\mathbf{r}_{ij}^T/r_{ij}^2)]$ for $i \neq j$, where $\mathbf{r}_{ij} \equiv \mathbf{r}_i - \mathbf{r}_j$, and $\mathbf{G}_{ii} = i(\Gamma/2)\mathbb{1}_3$ for the single-atom term, with $\Gamma = d_0^2 k^3/3\pi\epsilon_0\hbar$ the single-atom spontaneous decay rate, ϵ_0 free space permittivity, d_0 the transition dipole moment, and $k = \omega_0/c = 2\pi/\lambda$ its wave number. The elastic and inelastic terms of the dipolar interaction can be written as $\Delta^{ij} \equiv \hat{\epsilon}_i^* \cdot \mathrm{Re}\{\mathbf{G}_{ij}\} \cdot \hat{\epsilon}_j$ and $\Gamma^{ij} \equiv \hat{\epsilon}_i^* \cdot 2\mathrm{Im}\{\mathbf{G}_{ij}\} \cdot \hat{\epsilon}_j$, where $\hat{\epsilon}_i$ is the polarization of the ith dipole, which we choose to be $\hat{\epsilon}_i = \hat{\epsilon} = \hat{z}$. We have here considered a regular chain of atoms of spacing d along $\hat{x}$, with an incident laser propagating along $\mathbf{k} = k\hat{y}$ and polarized along $\hat{z}$ [see Fig. 2(a)]. In this configuration, the atoms couple only through the z polarization.

Collective effects have been studied extensively in the low-excitation limit (linear-optics) regime, with reports on collective frequency shifts, sub-, and superradiance [12,30–34]. The superradiant (SR) state in this context, also labeled the timed Dicke state [35], can be identified precisely by diagonalizing the single-excitation (linear-optics) coupling matrix $M^{ij} \equiv \Gamma^{ij} + i\Delta^{ij}$ [36–39]: it corresponds to the eigenstate whose eigenvalue has the largest real part, Γ_{SR}, while its imaginary part corresponds to its energy Δ_{SR} with respect to the atomic transition [40].

The generalization of the protocol presented in Fig. 1(b) to $N > 2$ consists in addressing a single superradiant eigenstate of the interacting Hamiltonian. In our setup, this is achieved by a homogeneous in-phase illumination by the drive and matching the laser detuning precisely to the interaction shift, $\Delta = \Delta_{\mathrm{SR}}$. A significant blockade effect requires a large energy shift, thus a small lattice spacing, and a Rabi frequency larger than the decoherence rate ($\Omega > \Gamma_{\mathrm{SR}}$). Here we chose $\Omega = 0.1\Delta_{\mathrm{SR}}$.

The resulting dynamics is illustrated in Fig. 2(c) for the case of $N = 4$ atoms spaced by $d = 0.1k^{-1}$, where we show the total excited population $n = \sum_{i=1}^N \langle \hat{n}_i \rangle$, with $\hat{n}_i = \hat{\sigma}_i^+ \hat{\sigma}_i^-$, as a function of time. We first notice that n is always less than unity and the inset plot confirms that the probability $P_{n\geq 2}$ of having more than one excitation in the system is very small ($\lesssim 10^{-2}$). The amplitude of these oscillations is

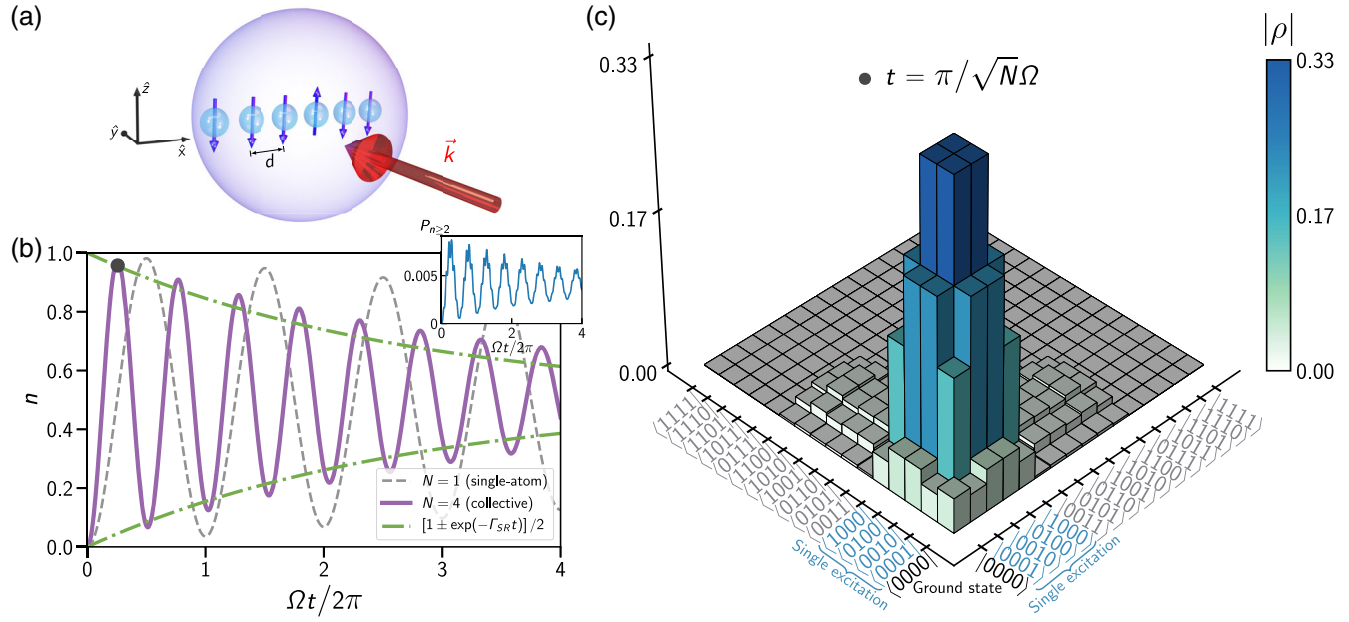

FIG. 2. (a) Regular chain of two-level atoms with spacing d along $\hat{x}$ and incident laser of wave vector $\mathbf{k} = k\hat{y}$, polarized along $\hat{z}$. The strong dipole-dipole interaction generates a large energy shift of the superradiant state, which permits the blockade effect (purple sphere). (b) Dynamics of the excited population n for $N = 1$ (dashed gray line) and $N = 4$ atoms (purple line), for a driving Rabi frequency $\Omega/\Gamma = 65$. For the $N = 1$ case, the atom is driven at resonance ($\Delta = 0$). For $N = 4$, the detuning is chosen to drive the superradiant mode ($\Delta = \Delta_{SR}$), and the system is composed of a regular chain with spacing $kd = 0.1$. The inset shows the probability of having many excitations to be $\lesssim 10^{-2}$ throughout the evolution. (c) Density matrix for a chain with $N = 4$ atoms, with spacing $kd = 0.1$, driven by a laser with detuning $\Delta/\Gamma = 649$, matching the superradiant-mode shift, and with a Rabi frequency $\Omega/\Gamma = 65$.

damped by an exponential envelope (dot-dashed green lines) consistent with the dominating decay rate Γ_{SR}, indicating that we are addressing specifically the SR state. Second, we observe that the frequency of oscillation is twice as large as the one of a driven single-atom (orange dashed line), which is thus consistent with the $\sqrt{N}\Omega$ scaling of the collective Rabi oscillations.

Furthermore, the blockade effect is confirmed by examining the time evolution of the density matrix: the dynamics is the one of an effective two-level system composed of the ground-state and the SR state. At time $t = \pi/\sqrt{N}\Omega$, after switching on the pump, we reach a state with the largest probability of finding a single excitation, with large off-diagonal coherences, as shown in Fig. 2(b). This can be confirmed by a fidelity of $\mathcal{F} = \langle \mathrm{SR}|\hat{\rho}|\mathrm{SR}\rangle = 0.96$, where the SR state is obtained from the diagonalization of the single-excitation matrix M^{ij}. This analysis, combined with the fact that the multiexcitation states are practically not populated [see inset of Fig. 2(c)] confirms that the blockade regime is achieved.

In our 1D geometry the SR state is not exactly the symmetric, W-state $|W\rangle \equiv (1/\sqrt{N})\sum_{i=1}^{N}|g\ldots ge_i g\ldots g\rangle$. As can be observed in Fig. 2(b), due to the boundary conditions the coherences and populations in the single-excitation sector (blue states) have slightly different values for edge and center atoms. We have verified that this imbalance becomes negligible in a symmetric ring geometry [41], with the excitation blockade equally present. More generally, in a 2D subwavelength sample with a pump polarization orthogonal to the atomic plane, all atoms essentially couple to a single light mode and their spatial organization is not critical to achieve the blockade effect. Since it relies on a strong energy shift of the SR, the blockade is guaranteed by our choice of a subwavelength lattice spacing ($kd \sim 0.1$), where the near-field $1/r^3$ terms dominate the dipolar interactions. Apart from the ring geometry discussed above, we have checked that the blockade is robust to disorder in the chain (inducing fluctuations of up to $0.5d$ on the atom positions in the plane orthogonal to the polarization) or to a vacancy in the chain (removing one atom at random from the chain): all these cases presented probability of having multiple excitations of less than 1% (not shown here).

Furthermore, our geometry couples dipoles with a polarization orthogonal to the atomic chain (see Fig. 2), yet the coupling could be tuned turning the linear polarization around $\mathbf{k}$, as encoded in the Green's tensor $\mathbf{G}_{ij}$. For example, the near-field terms cancel at the "magic angle" $\theta = \cos^{-1}(1/\sqrt{3})$ between the chain axis and the polarization, and change sign at this value. Note that 3D samples, or any configuration that mixes polarizations, require including the different scattering channels in the modeling, or alternatively imposing an external field to decouple these channels.

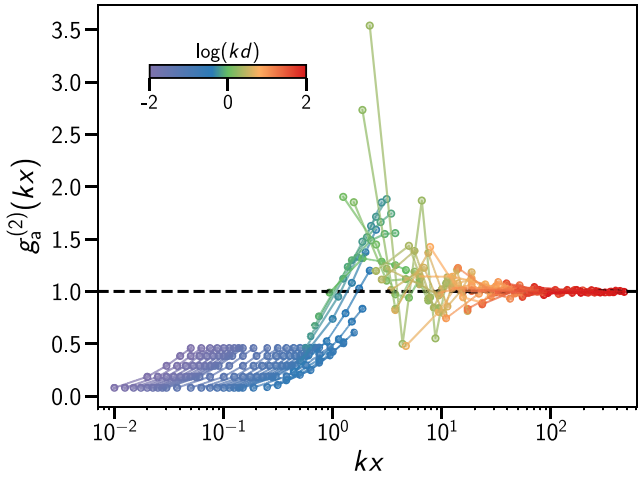

FIG. 3. Atomic pair correlation $g_a^{(2)}$ as a function of the lattice step x for chains of $N = 6$ atoms apart by different values of lattice spacing d.

We now proceed to discuss a blockade radius, which describes the distance within which atoms are expected to mutually induce a blockade of excitations. To this end, we introduce an average atomic pair correlation function [42,43]

$$g_a^{(2)}(s) = \frac{1}{N_s}\sum_i \frac{\langle \hat{n}_i \hat{n}_{i+s}\rangle}{\langle \hat{n}_i\rangle\langle \hat{n}_{i+s}\rangle}, \tag{4}$$

where N_s corresponds to the number of sites in the chain that are distant by s sites. As can be observed in Fig. 3, $g_a^{(2)}$ is below unity for atoms closer than $1/k$, indicating that excitations are blocked; it increases above unity as the sample size is of order of the wavelength, presenting an antiblockade (also known as excitation facilitating) regime [44–47]. This allows to define a blockade radius of $\sim 1/k$ for induced dipole interactions.

While probing directly the states of a subwavelength sample remains a huge challenge, photon blockade also leaves a direct signature on the scattered light. Apart from the collective Rabi oscillations discussed before, its signature can be found in the normalized intensity-intensity correlations of light [48]

$$g_l^{(2)}(\tau) \equiv \lim_{t\to\infty} \frac{\langle \hat{E}^-(t)\hat{E}^-(t+\tau)\hat{E}^+(t+\tau)\hat{E}^+(t)\rangle}{\langle \hat{E}^-(t)\hat{E}^+(t)\rangle^2}, \tag{5}$$

where we have used normal ordering for $g_l^{(2)}$. The electric field was computed using the far-field expression for the scattered field $\hat{E}^+ \sim \sum_{j=1}^N e^{-ik\hat{n}.\mathbf{r}_j}\hat{\sigma}_j^-$, in the direction $\hat{n} = \hat{y}$, where it has the polarization $(\hat{n}\times\hat{e})\times\hat{n} = \hat{z}$ of the incident laser. Here the contribution of the incident laser has been discarded: this corresponds to observing the emitted light a few degrees off the laser axis, which yields similar results since we are considering subwavelength samples.

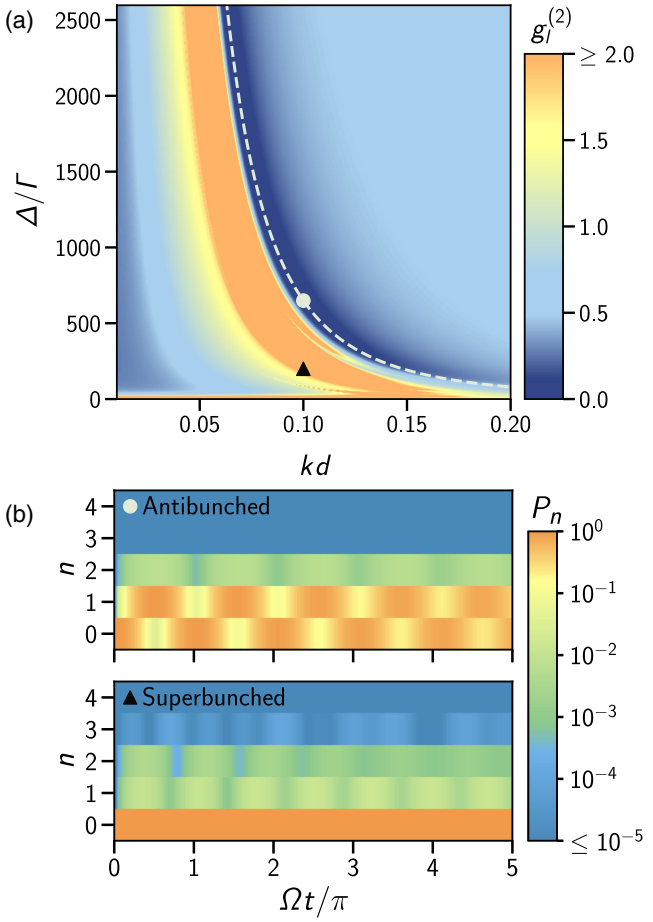

FIG. 4. (a) Map of second-order correlation function $g_l^{(2)}(0)$ for the light field scattered by a chain with $N = 4$ as a function of detuning Δ and spacing kd. The strongly antibunched states lie on top of the dark-blue area, which closely coincides with the single-excitation, superradiant energy shift (dashed white line [51]) for each spacing kd. (b) Probability P_n of exciting n atoms as a function of time for two cases highlighted in (a) (white dot and black triangle, respectively) an antibunched (photon-blockaded) state (top) with $g_l^{(2)}(0) = 0.03$ and a superbunched state (bottom) with $g_l^{(2)}(0) = 5.13$.

The light statistics describe photon bunching when $g_l^{(2)}(0) > 1$, superbunching for $g_l^{(2)}(0) > 2$ and antibunching (or photon blockade) when $g_l^{(2)}(0) < 1$ [49]—the latter necessarily implying nonclassicality [50]. A map of the $g_l^{(2)}(0)$ is presented in Fig. 4(a): we have checked that the values much smaller than unity correspond to the excitation-blockade regime [51], where the system oscillates between ground and single-excitation states [50]. This map shows with which driving frequency the SR state should be addressed for different lattice spacing (see dark blue region corresponding to the antibunching of photons and dashed white line describing the superradiant energy shift [51]). The detuning required to reach the photon-blockade region follows a $1/(kd)^3$ decay, as one expected from the

dominating term of the dipolar interactions at short distances.

The interactions that allow for the blockade regime generate other kinds of collective states. This is already visible from the analysis of the $g_l^{(2)}(0)$ in Fig. 4(a), where superbunching is observed (orange region). To illustrate this point, the probability P_n of exciting n atoms is monitored as a function of time: the blockade regime is characterized by a population that oscillates between the ground- and single-excitation states [see Fig. 4(b)]. The probability to explore a multiexcited state is comparatively small, and in phase with the single-excitation state, which suggests there are off-resonant events directly resulting from the SR state excitation. In contrast, driving the system at a different frequency can lead to a weakly excited ($P_0 \approx 1$) yet superbunched state [see Fig. 4(a)], where the single- and double-excitation states have comparable probabilities to be explored [51].

In conclusion, we have shown photon blockade using ground-state neutral atoms in subwavelength lattices by addressing a collective SR state of the system, whose energy can be shifted far away from the atomic resonance by induced dipole-dipole interactions. This protocol can be, in principle, implemented using atoms with long-lived clock transitions, which are considerably less sensitive to stray magnetic and electric fields than Rydberg atoms, offering robustness for coherent control. Note that while we have here used the SR state, a wealth of collective states is actually generated by the dipole-dipole interactions, including single-excitation subradiant states which are other candidates for excitation blockade [52]. Current progress in the experimental realization of subwavelength optical lattices holds many promises for creating and manipulating highly entangled states [24–26,53], opening the way for a possible implementation of the proposal discussed in this work. Note that our scheme is not limited to atomic setups, but also for other platforms being able to implement large dipole densities at subwavelength scales, such as with color centers [54–57] and light-harvesting complexes [58].

We thank Ana Maria Rey, Tommaso Macrì, Mathilde Hugbart, and William Guerin for helpful discussions. A. C., T. S. d. E. S., and R. B. are supported by FAPESP through Grants No. 2017/09390-7, No. 2018/12653-2, No. 2018/01447-2, No. 2018/15554-5, and No. 2019/13143-0. R. B. received support from the National Council for Scientific and Technological Development (CNPq) Grants No. 302981/2017-9 and No. 409946/2018-4. J. S. is supported by the French National Research Agency (ANR) through the Programme d'Investissement d'Avenir under Contract No. ANR-11-LABX-0058_NIE within the Investissement d'Avenir program ANR-10-IDEX-0002-02. Part of this work was performed in the framework of the European Training Network ColOpt, which is funded by the European Union (EU) Horizon 2020 programme under the Marie Sklodowska-Curie action, Grant Agreement No. 721465 and the ERC Advanced Grant No. 832219 (ANDLICA). R. B. and R. K. received support from project CAPES-COFECUB (Ph879-17/CAPES 88887.130197/2017-01) and from the French National Research Agency (ANR19-CE47-0014-01).

Note added in proof.—Recently, we became aware of concomitant work on related photon blockade with atomic arrays in Ref. [52].

[1] M. Saffman, T. G. Walker, and K. Mølmer, Rev. Mod. Phys. **82**, 2313 (2010).
[2] M. Saffman, J. Phys. B **49**, 202001 (2016).
[3] A. Omran, H. Levine, A. Keesling, G. Semeghini, T. T. Wang, S. Ebadi, H. Bernien, A. S. Zibrov, H. Pichler, S. Choi, J. Cui, M. Rossignolo, P. Rembold, S. Montangero, T. Calarco, M. Endres, M. Greiner, V. Vuletić, and M. D. Lukin, Science **365**, 570 (2019).
[4] C. Zhang, F. Pokorny, W. Li, G. Higgins, A. Pöschl, I. Lesanovsky, and M. Hennrich, Nature (London) **580**, 345 (2020).
[5] M. Saffman and T. G. Walker, Phys. Rev. A **72**, 022347 (2005).
[6] A. Arias, G. Lochead, T. M. Wintermantel, S. Helmrich, and S. Whitlock, Phys. Rev. Lett. **122**, 053601 (2019).
[7] E. A. Goldschmidt, T. Boulier, R. C. Brown, S. B. Koller, J. T. Young, A. V. Gorshkov, S. L. Rolston, and J. V. Porto, Phys. Rev. Lett. **116**, 113001 (2016).
[8] N. Takei, C. Sommer, C. Genes, G. Pupillo, H. Goto, K. Koyasu, H. Chiba, M. Weidemüller, and K. Ohmori, Nat. Commun. **7**, 13449 (2016).
[9] M. Mizoguchi, Y. Zhang, M. Kunimi, A. Tanaka, S. Takeda, N. Takei, V. Bharti, K. Koyasu, T. Kishimoto, D. Jaksch *et al.*, Phys. Rev. Lett. **124**, 253201 (2020).
[10] M. J. Martin, M. Bishof, M. D. Swallows, X. Zhang, C. Benko, J. von Stecher, A. V. Gorshkov, A. M. Rey, and J. Ye, Science **341**, 632 (2013).
[11] C. Qu and A. M. Rey, Phys. Rev. A **100**, 041602(R) (2019).
[12] W. Guerin, M. O. Araújo, and R. Kaiser, Phys. Rev. Lett. **116**, 083601 (2016).
[13] A. Asenjo-Garcia, M. Moreno-Cardoner, A. Albrecht, H. J. Kimble, and D. E. Chang, Phys. Rev. X **7**, 031024 (2017).
[14] A. Asenjo-Garcia, H. J. Kimble, and D. E. Chang, Proc. Natl. Acad. Sci. U.S.A. **116**, 25503 (2019).
[15] M. Moreno-Cardoner, D. Plankensteiner, L. Ostermann, D. E. Chang, and H. Ritsch, Phys. Rev. A **100**, 023806 (2019).
[16] J. A. Needham, I. Lesanovsky, and B. Olmos, New J. Phys. **21**, 073061 (2019).
[17] K. Ballantine and J. Ruostekoski, Phys. Rev. Research **2**, 023086 (2020).
[18] P.-O. Guimond, A. Grankin, D. V. Vasilyev, B. Vermersch, and P. Zoller, Phys. Rev. Lett. **122**, 093601 (2019).
[19] G. S. Agarwal and K. T. Kapale, J. Phys. B **39**, 3437 (2006).
[20] J. Cho, Phys. Rev. Lett. **99**, 020502 (2007).
[21] D. D. Yavuz and N. A. Proite, Phys. Rev. A **76**, 041802(R) (2007).
[22] A. V. Gorshkov, L. Jiang, M. Greiner, P. Zoller, and M. D. Lukin, Phys. Rev. Lett. **100**, 093005 (2008).
[23] J. A. Miles, Z. J. Simmons, and D. D. Yavuz, Phys. Rev. X **3**, 031014 (2013).

[24] Y. Wang, S. Subhankar, P. Bienias, M. Lacki, T.-C. Tsui, M. A. Baranov, A. V. Gorshkov, P. Zoller, J. V. Porto, and S. L. Rolston, Phys. Rev. Lett. **120**, 083601 (2018).
[25] S. Subhankar, P. Bienias, P. Titum, T.-C. Tsui, Y. Wang, A. V. Gorshkov, S. L. Rolston, and J. V. Porto, New J. Phys. **21**, 113058 (2019).
[26] T.-C. Tsui, Y. Wang, S. Subhankar, J. V. Porto, and S. L. Rolston, Phys. Rev. A **101**, 041603(R) (2020).
[27] M. J. Stephen, J. Chem. Phys. **40**, 669 (1964).
[28] R. H. Lehmberg, Phys. Rev. A **2**, 883 (1970).
[29] R. Friedberg, S. Hartmann, and J. Manassah, Phys. Rep. **7**, 101 (1973).
[30] T. Bienaimé, N. Piovella, and R. Kaiser, Phys. Rev. Lett. **108**, 123602 (2012).
[31] J. Pellegrino, R. Bourgain, S. Jennewein, Y. R. P. Sortais, A. Browaeys, S. D. Jenkins, and J. Ruostekoski, Phys. Rev. Lett. **113**, 133602 (2014).
[32] M. O. Araújo, I. Krešić, R. Kaiser, and W. Guerin, Phys. Rev. Lett. **117**, 073002 (2016).
[33] S. J. Roof, K. J. Kemp, M. D. Havey, and I. M. Sokolov, Phys. Rev. Lett. **117**, 073003 (2016).
[34] W. Guerin and R. Kaiser, Phys. Rev. A **95**, 053865 (2017).
[35] M. O. Scully, E. S. Fry, C. H. Raymond Ooi, and K. Wódkiewicz, Phys. Rev. Lett. **96**, 010501 (2006).
[36] A. Goetschy and S. E. Skipetrov, Phys. Rev. E **84**, 011150 (2011).
[37] A. Goetschy and S. E. Skipetrov, Europhys. Lett. **96**, 34005 (2011).
[38] S. E. Skipetrov and I. M. Sokolov, Phys. Rev. Lett. **112**, 023905 (2014).
[39] L. Bellando, A. Gero, E. Akkermans, and R. Kaiser, Phys. Rev. A **90**, 063822 (2014).
[40] T. S. do Espirito Santo, P. Weiss, A. Cipris, R. Kaiser, W. Guerin, R. Bachelard, and J. Schachenmayer, Phys. Rev. A **101**, 013617 (2020).
[41] J. Cremer, D. Plankensteiner, M. Moreno-Cardoner, L. Ostermann, and H. Ritsch, New J. Phys., https://doi.org/10.1088/1367-2630/aba4d4.
[42] C. Ates, T. Pohl, T. Pattard, and J. M. Rost, J. Phys. B **39**, L233 (2006).
[43] H. Labuhn, D. Barredo, S. Ravets, S. de Léséleuc, T. Macrì, T. Lahaye, and A. Browaeys, Nature (London) **534**, 667 (2016).
[44] C. Ates, T. Pohl, T. Pattard, and J. M. Rost, Phys. Rev. Lett. **98**, 023002 (2007).
[45] T. M. Weber, M. Höning, T. Niederprüm, T. Manthey, O. Thomas, V. Guarrera, M. Fleischhauer, G. Barontini, and H. Ott, Nat. Phys. **11**, 157 (2015).
[46] F. Letscher, O. Thomas, T. Niederprüm, M. Fleischhauer, and H. Ott, Phys. Rev. X **7**, 021020 (2017).
[47] D. Kara, A. Bhowmick, and A. K. Mohapatra, Sci. Rep. **8**, 5256 (2018).
[48] A. Eloy, Z. Yao, R. Bachelard, W. Guerin, M. Fouché, and R. Kaiser, Phys. Rev. A **97**, 013810 (2018).
[49] D. F. Walls and G. J. Milburn, *Quantum Optics* (Springer Science & Business Media, Berlin, 2007).
[50] H. J. Kimble, M. Dagenais, and L. Mandel, Phys. Rev. Lett. **39**, 691 (1977).
[51] See Supplemental Material at http://link.aps.org/supplemental/10.1103/PhysRevLett.125.073601 for videos with the evolution of the density matrices of the selected anti- and superbunched states, analytical derivation of the superradiant energy shift ($N = 4$), and maps with correspondence between regimes of excitation blockade and photon antibunching.
[52] L. Williamson, M. Borgh, and J. Ruostekoski, following Letter, Superatom Picture of Collective Nonclassical Light Emission and Dipole Blockade in Atom Arrays, Phys. Rev. Lett. **125**, 073602 (2020).
[53] J. Rui, D. Wei, A. Rubio-Abadal, S. Hollerith, J. Zeiher, D. M. Stamper-Kurn, C. Gross, and I. Bloch, Nature (London) **583**, 369 (2020).
[54] P. C. Maurer, J. R. Maze, P. L. Stanwix, L. Jiang, A. V. Gorshkov, A. A. Zibrov, B. Harke, J. S. Hodges, A. S. Zibrov, A. Yacoby, D. Twitchen, S. W. Hell, R. L. Walsworth, and M. D. Lukin, Nat. Phys. **6**, 912 (2010).
[55] M. L. Juan, C. Bradac, B. Besga, M. Johnsson, G. Brennen, G. Molina-Terriza, and T. Volz, Nat. Phys. **13**, 241 (2017).
[56] C. Bradac, M. T. Johnsson, M. v. Breugel, B. Q. Baragiola, R. Martin, M. L. Juan, G. K. Brennen, and T. Volz, Nat. Commun. **8**, 1205 (2017).
[57] G. Rainò, M. A. Becker, M. I. Bodnarchuk, R. F. Mahrt, M. V. Kovalenko, and T. Stöferle, Nature (London) **563**, 671 (2018).
[58] H. Dong, S.-W. Li, Z. Yi, G. S. Agarwal, and M. O. Scully, arXiv:1608.04364.